

# Cosmological constraints from angular homogeneity scale measurements

Xiaoyun Shao<sup>1,\*</sup>, Carlos A. P. Bengaly<sup>1,†</sup>, Rodrigo S. Gonçalves<sup>1,2,‡</sup>, Gabriela C. Carvalho<sup>3,§</sup> and Jailson Alcaniz<sup>1,¶</sup>

<sup>1</sup>*Observatório Nacional, 20921-400, Rio de Janeiro, RJ, Brazil*

<sup>2</sup>*Departamento de Física, Universidade Federal Rural do Rio de Janeiro, 23897-000, Seropédica, RJ, Brazil and*

<sup>3</sup>*Faculdade de Tecnologia, Universidade do Estado do Rio de Janeiro, 27537-000, Resende, RJ, Brazil*

(Dated: September 11, 2024)

In this paper, we obtain new measurements of the angular homogeneity scale ( $\theta_H$ ) from the BOSS DR12 and eBOSS DR16 catalogs of Luminous Red Galaxies of the Sloan Digital Sky Survey. Considering the flat  $\Lambda$ CDM model, we use the  $\theta_H(z)$  data to constrain the matter density parameter ( $\Omega_{m0}$ ) and the Hubble constant ( $H_0$ ). We find  $H_0 = 65.7 \pm 7.0$  km s<sup>-1</sup> Mpc<sup>-1</sup> and  $\Omega_{m0} > 0.293$ . By combining the  $\theta_H$  measurements with current Baryon Acoustic Oscillations (BAO) and Type Ia Supernova (SN) data, we obtain  $H_0 = 69.9^{+4.9}_{-4.5}$  km s<sup>-1</sup> Mpc<sup>-1</sup> and  $\Omega_{m0} = 0.294^{+0.013}_{-0.015}$  ( $\theta_H$  + BAO) and  $H_0 = 70.7^{+5.2}_{-4.1}$  km s<sup>-1</sup> Mpc<sup>-1</sup> and  $\Omega_{m0} = 0.299 \pm 0.022$  ( $\theta_H$  + SN). We show that  $\theta_H$  measurements help break the BAO and SN degeneracies concerning  $H_0$ , as they do not depend on the sound horizon scale at the drag epoch or the SN absolute magnitude value obtained from the distance ladder method. Hence, despite those constraints being loose compared to other probes,  $\theta_H$  data may provide an independent cosmological probe of  $H_0$  in light of the Hubble tension. For completeness, we also forecast the constraining power of future  $\theta_H$  data via Monte Carlo simulations. Considering a relative error of the order of 1%, we obtain competitive constraints on  $\Omega_{m0}$  and  $H_0$  ( $\approx$  5% error) from the joint analysis with current SN and BAO measurements.

## I. INTRODUCTION

The standard cosmological model (SCM) consists on the  $\Lambda$ -Cold Dark Matter ( $\Lambda$ CDM) scenario, which describes an Universe undergoing a late-time accelerated phase, and whose physical nature of its dominating components, i.e., the cold dark matter (CDM) and the Cosmological Constant ( $\Lambda$ ), are still unknown to this date. Although this model can successfully explain a variety of cosmological observations, such as the Cosmic Microwave Background (CMB), the clustering of weak lensing of large scale structures (LSS), and the distances to standardizable candles like Type Ia Supernovae (SN) [1–6], it is plagued with several theoretical caveats, e.g. coincidence and fine-tuning problems [7], in addition to recent observational issues, such as the  $\sim 5\sigma$  tension between early and late-time measurements of the Hubble constant (see e.g. [8] and references therein). Recently, the results from the first data release of the Dark Energy Spectroscopic Instrument (DESI) hinted at a potential evidence for dynamical dark energy, instead of a Cosmological Constant [9] (see also [10]), yet this result has been under debate [11, 12].

Thus, it is crucial to test the fundamental assumptions of the SCM, since any significant departure from their assumptions would require a complete reformulation of such paradigm. One of these hypothesis is the Cosmological Principle (CP), which states that spatially the Universe looks statistically homogeneous and isotropic

at sufficiently large scales [13–16]. As a consequence, we can describe cosmological distances and ages by means of the Friedmann-Lemaître-Robertson-Walker (FLRW), as in the case of the SCM [17, 18]. We can verify this assumption by measuring the so-called cosmic homogeneity scale, which is defined as a characteristic scale where the large scale structure of the Universe, as observed by biased dark matter tracers such as galaxies and quasars, looks statistically indistinguishable from a random distribution – which is statistically homogeneous and isotropic by construction, being limited only by shot (Poisson) noise.

Given this motivation, extensive analyses have been carried out in order to identify and measure such scale, hereafter denoted by  $R_H$ . Most of them could positively identify such scale, and reported that  $R_H$  should be around 70–150 Mpc, using a variety of galaxy and quasar catalogues from large redshift surveys [19–29]. However, some works dispute this result [30–32], or argued that those measurements could be biased by the survey window function [33]. Moreover, it is possible to measure  $\theta_H$ , i.e., the two-dimensional (2D) measure of the homogeneity scale, given only in terms of the source position in the sky [34]. This approach has the advantage of avoiding the assumption of a cosmological model to convert redshift into distances, as required for its three-dimensional counterpart,  $R_H$ . This angular homogeneity scale  $\theta_H$  was successfully identified and measured using different redshift survey catalogues [35–37].

Recently, it was proposed that the 3D homogeneity scale  $R_H$  could be used as a sort of standard ruler, in a similar fashion to the sound horizon scale in baryon acoustic oscillations measurements (BAO) [38, 39]. However, a subsequent paper showed that such scale cannot provide a valid standard ruler, due to its nonmonotonic relation with the matter density parameter [40]. This

\*Electronic address: xiaoyun48@on.br

†Electronic address: carlosbengaly@on.br

‡Electronic address: rsousa@on.br

§Electronic address: gabriela.coutinho@fat.uerj.br

¶Electronic address: alcaniz@on.br

result was later confirmed in [41]. On the other hand, it was also shown in [41] that the angular homogeneity scale  $\theta_H$  could be a feasible standard ruler, as it does not exhibit such nonmonotonic behaviour with respect to the matter density, as well as the Hubble Constant. Hence, it is possible to use its measurements at different redshifts to constrain these parameters, as done using the latest  $\theta_H$  measurements provided by [37] in the same work.

In this paper, we extend the cosmological constraints analysis carried out in [41]. We do so by re-analyzing the  $\theta_H$  measurements obtained in [36] as well as in [37] with the former obtained from the SDSS-III BOSS DR12 CMASS galaxy sample of Luminous Red Galaxies (LRGs), and the later from the aforementioned SDSS-IV eBOSS DR16 LRG measurements, covering at the total the redshift range  $0.46 \leq z \leq 0.74$ . Then, we investigate the constraints obtained by combining those measurements with other cosmological data-sets, e.g. SN and BAO, and quantify the constraints that future  $\theta_H$  measurements, as expected with the advent of ongoing and upcoming redshift surveys, will be able to impose.

This paper is organized as follows: In Section II we describe the observational data utilized in our analysis. In Section III, we present our methodology and our set of angular homogeneity scale measurements. In Section IV, we show the results of our cosmological analysis, and we present our conclusions and final remarks in Section V.

## II. DATA

The Sloan Digital Sky Survey (SDSS) is a global scientific collaboration that has produced highly accurate three-dimensional maps of the Universe. The project was partitioned into four distinct phases: SDSS-I (2000-2005), SDSS-II (2005-2008), SDSS-III (2008-2014), and SDSS-IV (2014-2020). This study focuses on the Data Release 12 (DR12) of the Baryon Oscillation Spectroscopic Survey (BOSS) [42–44], and the Data Release 16 (DR16) of the extended Baryon Oscillation Spectroscopic Survey (eBOSS) [45], which are subsets of the Sloan Digital Sky Survey III (SDSS-III) and Sloan Digital Sky Survey IV (SDSS-IV), respectively.

Specifically this work adopts the northern sky of both BOSS DR12 and eBOSS DR16 catalogues of Luminous Red Galaxies and for the sake of simplicity we hereafter name them as DR12 and DR16, respectively. The exclusion of the southern sky subsample is due to the limited sky coverage.

The main features of the DR12 and DR16 data set used in this work are shown in Table I and Table II, respectively. The redshift interval in each dataset is  $0.46 < z < 0.62$  with around 420,000 points (DR12) and  $0.67 < z < 0.74$  with approximately 30,000 points (DR16), as displayed in Fig.1. The footprint of the sky area coverage of both catalogues is shown in Fig.2.

As we focus on measuring the angular scale of homo-

geneity, we split the data into redshift bins of  $\Delta z = 0.01$ . The size of the bin is chosen to avoid projection effects [46], so we can avoid possible biases on homogeneity scale measurements, and increase the number of data points, thus providing a good statistical performance for the analysis [27, 28, 34, 37].

Also, as shown in [41], the angular homogeneity scale exhibits a monotonical behavior for the matter density parameter and Hubble Constant in the range  $\Omega_{m0} \in [0.15, 0.8]$  and  $H_0 \in [40, 100]$  (hereafter given in units of  $\text{km s}^{-1} \text{Mpc}^{-1}$ , unless stated otherwise), respectively, and it is more sensitive to  $H_0$  than  $\Omega_{m0}$ . Thus, this quantity can be used as to constrain those parameters. In order to extend the monotonicity of angular homogeneity scale to lower redshifts, we reduce the range of  $\Omega_{m0}$  and  $H_0$ . We find that the angular homogeneity scale presents a monotonical behavior with  $\Omega_{m0} \in [0.15, 0.5]$  and  $H_0 \in [40, 80]$  for  $z \gtrsim 0.46$ . These intervals of  $\Omega_{m0}$  and  $H_0$  are well within the current uncertainties of their respective constraints obtained by CMB and SN observations, hence we can safely use LRGs within the redshift range  $0.46 < z < 0.74$  to perform our analysis.

TABLE I: The redshift bins adopted in our analysis from BOSS (DR12), along with the redshit bin means and corresponding number of LRGs in each bin.

$z$	$\bar{z}$	$N_{gal}$
0.46-0.47	0.465	22551
0.47-0.48	0.475	27319
0.48-0.49	0.485	29251
0.49-0.50	0.495	31763
0.50-0.51	0.505	33107
0.51-0.52	0.515	32887
0.52-0.53	0.525	32794
0.53-0.54	0.535	31995
0.54-0.55	0.545	31355
0.55-0.56	0.555	29486
0.56-0.57	0.565	28995
0.57-0.58	0.575	25289
0.58-0.59	0.585	23997
0.59-0.60	0.595	22568
0.60-0.61	0.605	20594
0.61-0.62	0.615	18799

TABLE II: The redshift bins adopted in our analysis from eBOSS (DR16), along with the redshit bin means and corresponding number of LRGs in each bin.

$z$	$\bar{z}$	$N_{gal}$
0.67-0.68	0.675	4073
0.68-0.69	0.685	4222
0.69-0.70	0.695	4064
0.70-0.71	0.705	4209
0.71-0.72	0.715	4239
0.72-0.73	0.725	4084
0.73-0.74	0.735	4210

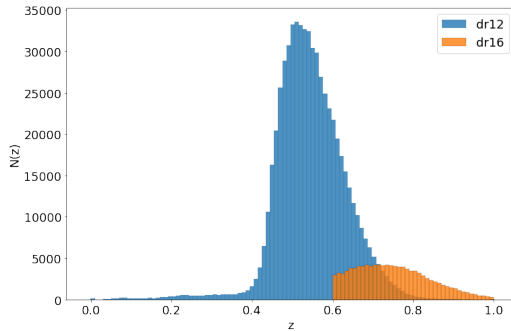


FIG. 1: Redshift distributions of the LRGs from BOSS DR12 and eBOSS DR16 catalogues. We considered the redshift range  $0.46 < z < 0.74$ .

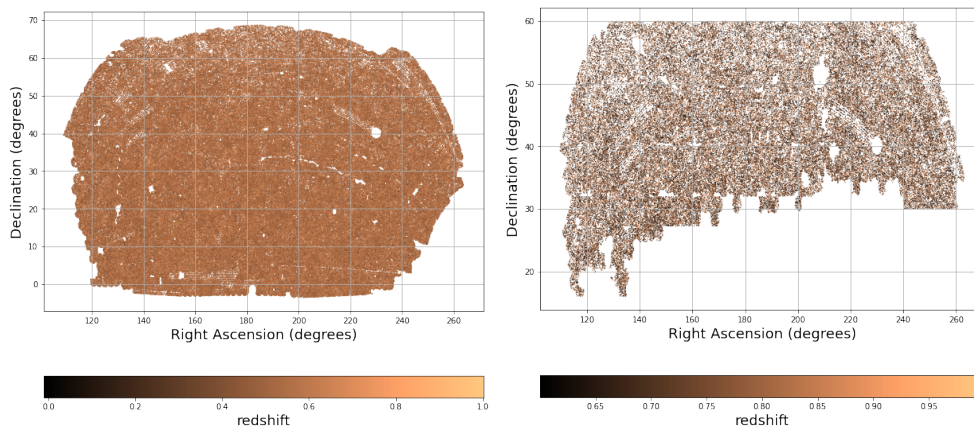


FIG. 2: The footprint of DR12 and DR16, respectively

### III. METHODOLOGY

#### A. Theoretical framework

In this section, we make an overview of the method that was developed to use the angular homogeneity scale  $\theta_H$  as a standard ruler. For a careful description, we refer the reader to [41], where this method is fully described.

The fractal dimension  $D_2$  is the key quantity needed to measure the angular homogeneity scale of the data, and thus constrain cosmological parameters (see e.g. [19–41] and references therein). As we are performing a 2D analysis, the fractal dimension is defined over an angular separation  $\theta$ .

Numerically, we define that the angular homogeneity characteristic scale is reached where  $D_2$  approaches 1% of its expected value, following [21]. This implies that  $\theta_H$  represents the angular scale where  $D_2(\theta_H) = 1.98$ .

The expression for the fractal dimension is given by

$$D_2(\theta) = 2 + \frac{d \ln}{d \ln \theta} \left[ 1 + \frac{1}{1 - \cos \theta} \int_0^\theta \omega(\theta') \sin \theta' d\theta' \right], \quad (1)$$

where  $\omega(\theta)$  is the two-point angular correlation function

(2PCF), which can be expressed as [47]

$$\omega(\theta) = \int dz_1 f(z_1) \int dz_2 f(z_2) \xi(r(z_1), r(z_2), \theta, \bar{z}) \quad (2)$$

where the redshifts  $z_1$  and  $z_2$  define the limits of the correspondent spherical shell analyzed, and  $\xi$  is the three-dimensional two-point correlation function for matter, as described below. Also, we assume  $f(z) \equiv b(z)\phi(z)$ , where  $\phi(z)$  denotes the radial selection, i.e., the probability to include a galaxy in a given redshift bin, and  $b(z)$  is the bias parameter, which relates the galaxy distribution to the underlying matter distribution. To account for this bias, a linear bias model designed for the two-point correlation function is applied [48]

$$b(z; A, B) = A \left( \frac{1+z}{1+z_{\text{eff}}} \right)^B, \quad (3)$$

where  $z_{\text{eff}}$  represents the intermediate redshift bin value. The factor  $(1+z_{\text{eff}})$  is included in order to mitigate the degeneracy that exists between the parameters  $A$  and  $B$  [49].

In this paper, we consider only top-hat window functions and narrow redshift bins, so we compute the 2PCF and the 3D correlation function for matter as

$$\xi(r) = \frac{1}{2\pi^2} \int_0^\infty j_0(kr) k^2 P(k) dk, \quad (4)$$

where  $P(k)$  is the matter power spectrum and  $j_0(x) = \sin(x)/x$ . Also, the comoving distance to a certain redshift  $z$  is given by

$$r(z) = \int_0^z \frac{c}{H(z')} dz', \quad (5)$$

where

$$H(z) = H_0 \sqrt{\Omega_{m0}(1+z)^3 + (1-\Omega_{m0})}. \quad (6)$$

We use the CAMB code to calculate the theoretical prediction of the matter power spectrum  $P(k)$  [50]. As our focus is solely on large cosmological scales, we restrict our analysis to the linear segment of the spectrum. This assumption holds since we define a threshold of 1% for  $D_2$  in order to find  $\theta_H$  [39].

## B. Estimating $\theta_H$

The method above describes how to obtain the theoretical predictions of  $\theta_H$ . In what follows, we discuss how to estimate the relevant observational quantities to constrain the cosmological parameters.

We assume the Landy-Szalay 2PACF estimator,  $\hat{\omega}_{ls}(\theta)$  [51], which is obtained directly from a combination of the data and random catalogues [34, 36, 37]. It is defined as

$$\hat{\omega}_{ls}(\theta) = \frac{DD(\theta) - 2DR(\theta) + RR(\theta)}{RR(\theta)}, \quad (7)$$

where  $DD(\theta)$ ,  $DR(\theta)$ , and  $RR(\theta)$  are the numbers of pairs of data as a function of their separations  $\theta$ , normalized by the total number of pairs, in data-data, data-random and random-random catalogues, respectively. The pair-counting was done with the TREECORR package [52]. Concerning to the random catalogues, we use the BOSS and eBOSS catalogues, which are approximately 50 and 20 times larger than the respective real catalogues [42–45]. This ensures that the statistical fluctuations caused by the random points are insignificant.

Therefore, in order to calculate the  $D_2$  values and uncertainties, we perform the following steps: (i) we calculate the value of  $D_2$  using Eqs. 1 and 7 for different values of  $\theta$ ; (ii) we perform a polynomial fit, and determine the angular homogeneity scale  $\theta_H$  at the point where  $D_2 = 1.98$ ; (iii) we repeat this procedure 1000 times via bootstrap resampling technique, resulting in a distribution of  $\theta_H$  values; (iv) we calculate the mean and standard deviation of the values obtained in step (iii) as our measurements of the angular homogeneity scale and its corresponding uncertainty. The results are displayed in Table III and Table IV.

TABLE III: The redshift means,  $\bar{z}$  (each bin has a width of  $\Delta z = 0.01$ ) and the respective observational angular homogeneity scale,  $\theta_H^{boot}$ , obtained from the DR12 data set.

$\bar{z}$	$\theta_H(\text{degree})$
0.465	$10.4 \pm 2.47$
0.475	$10.43 \pm 2.58$
0.485	$9.70 \pm 2.73$
0.495	$9.08 \pm 2.50$
0.505	$9.14 \pm 2.48$
0.515	$9.28 \pm 2.76$
0.525	$9.57 \pm 2.39$
0.535	$9.80 \pm 2.67$
0.545	$9.72 \pm 2.69$
0.555	$9.17 \pm 2.54$
0.565	$9.35 \pm 2.77$
0.575	$9.07 \pm 2.75$
0.585	$8.31 \pm 2.63$
0.595	$8.88 \pm 2.87$
0.605	$8.54 \pm 2.90$
0.615	$8.36 \pm 2.90$

TABLE IV: Same as the previous table, but rather for the DR16 data set.

$\bar{z}$	$\theta_H^{boot}(\text{degree})$
0.675	$7.49 \pm 2.83$
0.685	$8.53 \pm 2.58$
0.695	$8.07 \pm 2.59$
0.705	$7.36 \pm 2.49$
0.715	$6.92 \pm 2.28$
0.725	$8.12 \pm 2.04$
0.735	$8.89 \pm 2.90$

## IV. COSMOLOGICAL ANALYSIS

We adopt the Monte Carlo Markov Chain (MCMC) method to constrain cosmological parameters from the angular homogeneity scale measurements  $\theta_H$ . We will now proceed with the next three steps. Initially, we conduct a MCMC analysis to solely the angular scale measurements. Secondly, we combine the  $\theta_H$  measurements with Supernovae and Baryon Acoustic Oscillations (BAO) data to understand the complementarity of these data and restrict the cosmological parameters  $\Omega_{m0}$  and  $H_0$ . In the third stage, we derive  $\theta_H$  points with smaller uncertainties by Monte Carlo Simulations to forecast the future constraining power of the data.

### A. Angular homogeneity scale measurements

We perform a Markov Chain Monte Carlo analysis to determine the constraints imposed by the angular homogeneity scale measurements on the cosmological parameter space  $p_C = (H_0, \Omega_m)$  in the framework of a spatially flat  $\Lambda$ CDM model. The  $\chi^2$  value that we investigate by means of a Markov Chain Monte Carlo (MCMC)

approach is defined as:

$$\chi^2 = \sum_{i=1}^N \left( \frac{\theta_H^G(z_i) - \theta_H^{G,th}(z_i; b, p_C, p_F)}{\sigma_{\theta_H^G}(z_i)} \right)^2 \quad (8)$$

where  $\theta_H^G$  and  $\sigma_{\theta_H^G}$  correspond to the observational homogeneity scale measurements and their corresponding errors, respectively, as shown in Table III and Table IV. On the other hand  $\theta_H^{G,th}$  is the prediction of the homogeneity scale of the galaxies distribution as a function of redshift ( $z_i$ ), the bias factor of the galaxies ( $b$ , as explicit in eq. (3)) and the set of free  $p_C$  and fixed  $p_F$  cosmological parameters. In the present work, we assume  $p_F$  as fiducial values from Planck 2018 [1], so that the free parameters in our analysis are  $\Omega_{m0}$ ,  $H_0$ ,  $A$  and  $B$ .

The results of the MCMC analysis are presented in Fig. 3. In the left panel of Fig. 3 we show the constraints imposed by the  $\theta_H$  measurements over the cosmological parameters  $\Omega_{m0}$  and  $H_0$  after marginalizing over the bias parameters  $A$  and  $B$ . We estimate  $H_0 = 65_{-5}^{+10}$  km.s<sup>-1</sup>.Mpc<sup>-1</sup>, which agrees with the best-fit from Planck CMB observations, although  $H_0$  measurements from SN are well within the  $1\sigma$  credible region. Besides,  $\Omega_{m0}$  is mostly unconstrained, i.e.,  $\Omega_{m0} > 2.93$ , in agreement with the results reported in [41].

We also investigate how these results may change when we fix the bias parameters  $A$  and  $B$  to the mean values ( $A = 2.6$  and  $B = 1.13$ ), obtained by MCMC analysis rather than marginalizing over them. The results are shown in the right panel of Fig. 3. Despite the fact that  $\Omega_{m0}$  is still unconstrained, we found  $H_0 = 65.7 \pm 7.0$  km.s<sup>-1</sup>.Mpc<sup>-1</sup>, so with a slightly improvement in comparison with the results shown in the left panel of Fig. 3.

## B. Joint analysis

This subsection discusses the joint constraints obtained from  $\theta_H$  and the Baryon Acoustic Oscillations (BAO) and Supernova (SN) observations. We perform such an analysis because  $\theta_H$  is more sensitive to  $H_0$  than  $\Omega_{m0}$ . In contrast, the opposite occurs for the other two probes – unless we specify priors on  $r_{drag}$  [53] and  $M_B$  [54], representing the sound horizon scale at drag epoch and the SN absolute magnitude, respectively. Hence, a joint analysis between  $\theta_H$  with BAO or SN may help break the well-known degeneracies between the  $H_0$  and  $r_{drag}$  in the BAO case and between  $H_0$  and  $M_B$  in the SN case. This kind of joint analysis could be significant in light of the  $\sim 5\sigma$  above tension between early- and late-time measurement of the Hubble Constant. However, we emphasize that our main focus here is to quantify the  $\theta_H$  performance on constraining the main background parameters of the standard cosmological model, i.e., the  $H_0$  than  $\Omega_{m0}$ , rather than trying to address this issue using the  $\theta_H$ . Such an analysis will be pursued in future work.

It is worth noting that, in this analysis, the bias parameters  $A$  and  $B$  are fixed at the mean values previously mentioned. We make this choice to dodge the degeneracy between those parameters and  $\Omega_{m0}$  and optimize the joint analyses.

The BAO dataset corresponds to a compilation of measurements obtained from the SDSS DR7 main galaxy sample [55], the 6dF galaxy survey [56], as well as the SDSS BOSS DR12 [57] and eBOSS DR16 surveys [58]. The result of the joint analysis between  $\theta_H$  and BAO data is shown in the left panel of Fig. 4, where we obtain the following constraints:  $H_0 = 69.9_{-4.5}^{+4.9}$  km.s<sup>-1</sup>.Mpc<sup>-1</sup> and  $\Omega_{m0} = 0.294_{-0.015}^{+0.013}$ . Our results demonstrate a significant improvement compared to those shown in Fig 3, as expected due to the small uncertainties in the BAO measurements. Also, we confirm that this combination of datasets can help break the BAO degeneracy with  $H_0$  since we did not assume the  $r_{drag}$  value here.

As for our SN sample, we use the Pantheon dataset, which comprises 1048 supernovae distributed across the redshift range of  $0.01 < z < 2.3$  [59]. The results of the combined  $\theta_H$  and SN samples are shown in the right panel of 4. As we can see, this combination leads to constraints such as  $H_0 = 70.7_{-4.1}^{+5.2}$  km.s<sup>-1</sup>.Mpc<sup>-1</sup> and  $\Omega_{m0} = 0.299 \pm 0.022$ ; hence, as in the BAO case, we find that this joint analysis helps break the SN degeneracy with  $H_0$ , since the latter constraints are independent of the SH0ES prior on  $M_B$ .

## C. Forecasting $\theta_H$

To investigate the constraining power of future  $\theta_H$  data on the cosmological parameters, we perform simulations of the angular homogeneity scale by assuming smaller uncertainties on its measurements via Monte Carlo Simulations. Firstly, we fit the observational relative errors ( $\varepsilon_{\theta_H} = \frac{\sigma_{\theta_H}}{\theta_H}$ ) from Table III and Table IV.

After that, we assume a smaller observational uncertainty in order to reproduce expectation values of future measurements. As an example, we choose  $\sigma_{\theta_H}^{sim} = 1\% \sigma_{\theta_H} \rightarrow \varepsilon_{\theta_H}^{sim} = 1\% \varepsilon_{\theta_H}$ . Afterwards, we then obtain the simulated values for  $\theta_H$  by sampling them from a Gaussian distribution with a functional form of  $N(\theta_H^{fid}, \sigma_{\theta_H}^{sim})$  at each redshift, where  $\theta_H^{fid}$  is obtained by assuming a fiducial cosmology model, and the uncertainty  $\sigma_{\theta_H}^{sim}$  is obtained as above described. We assume the flat- $\Lambda$ CDM best fit from Planck 2018 as fiducial model and generate data sets with the same features of the observational data, i.e., 23 points and the redshift range from 0.46 to 0.74. Then, in order to get the constraints on  $H_0$  and  $\Omega_{m0}$ , we perform a MCMC analysis using these simulated data, as in the case of the real data.

From the simulated  $\theta_H$  data alone, we obtain  $H_0 = 66 \pm 7$  km.s<sup>-1</sup>.Mpc<sup>-1</sup> and  $\Omega_{m0} = 0.351_{-0.045}^{+0.140}$  (Fig. 5). As expected, we find that, as the uncertainty of  $\theta_H$  decreases, the constraints imposed on  $H_0$  and  $\Omega_{m0}$  are

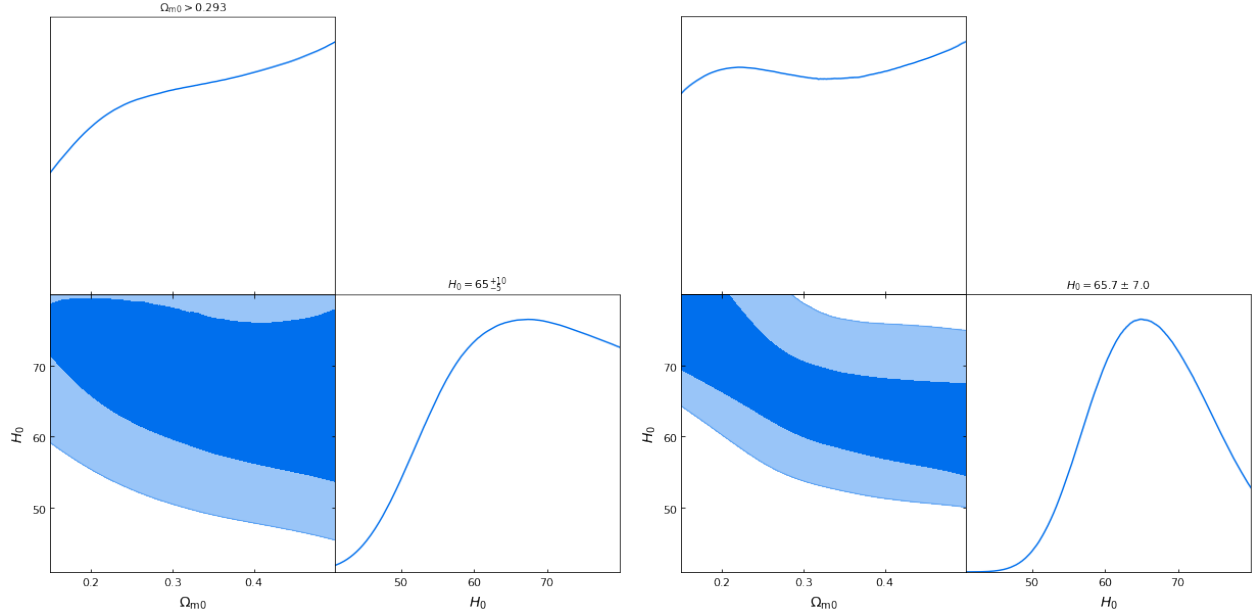


FIG. 3: The posteriors of  $\Omega_{m0}$  and  $H_0$  with 68% ( $1\sigma$ ) and 95% ( $2\sigma$ ) credible regions with the bias parameters  $A$  and  $B$  (left) being marginalized and (right) fixed at the mean values.

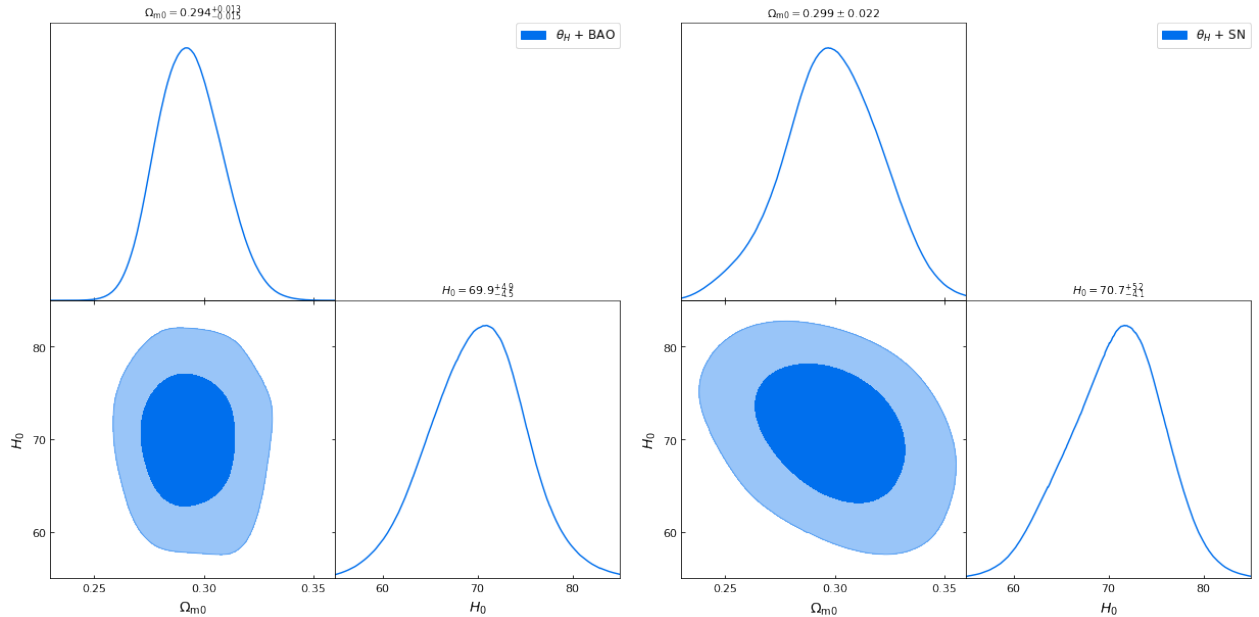


FIG. 4: Joint analysis contours of posteriors for  $\Omega_{m0}$  and  $H_0$ , with 68% and 95% credible regions, by combining the angular homogeneity scale estimations with BAO (left) and SN (right). In both cases we fix  $A$  and  $B$  at the mean values.

markedly improved – especially on the  $\Omega_{m0}$  parameter, as we obtain non-degenerated constraints of  $\Omega_{m0}$  in this case.

We separately perform a joint analysis of those simulated  $\theta_H$  realizations with the same BAO and SN external datasets. The results are shown in Fig. 6. In the left panel of Fig. 6, we present the constraints obtained from the  $\theta_H$  simulation combined with the BAO, i.e.,

$H_0 = 69.8 \pm 3.6 \text{ km.s}^{-1}.\text{Mpc}^{-1}$  and  $\Omega_{m0} = 0.293 \pm 0.014$ . Although the  $\Omega_{m0}$  constraint does not change significantly in this case, there is a notable improvement in the  $H_0$  estimate – thus helping break the BAO degeneracy between the Hubble Constant and sound horizon scale even further. On the other hand, the right panel of Fig. 6 shows the results obtained from the combination of the same simulated  $\theta_H$  data with the Pantheon

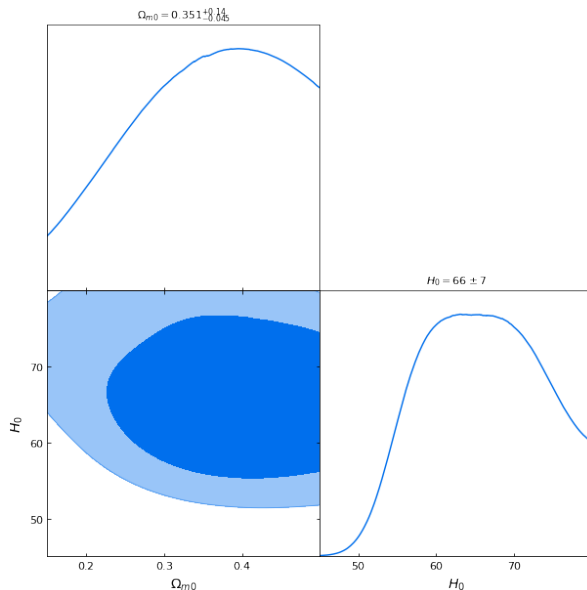


FIG. 5: The parametric space of  $H_0$  and  $\Omega_m$  obtained from the simulated data with 1% of current uncertainties, and with bias parameters  $A$  and  $B$  marginalized over.

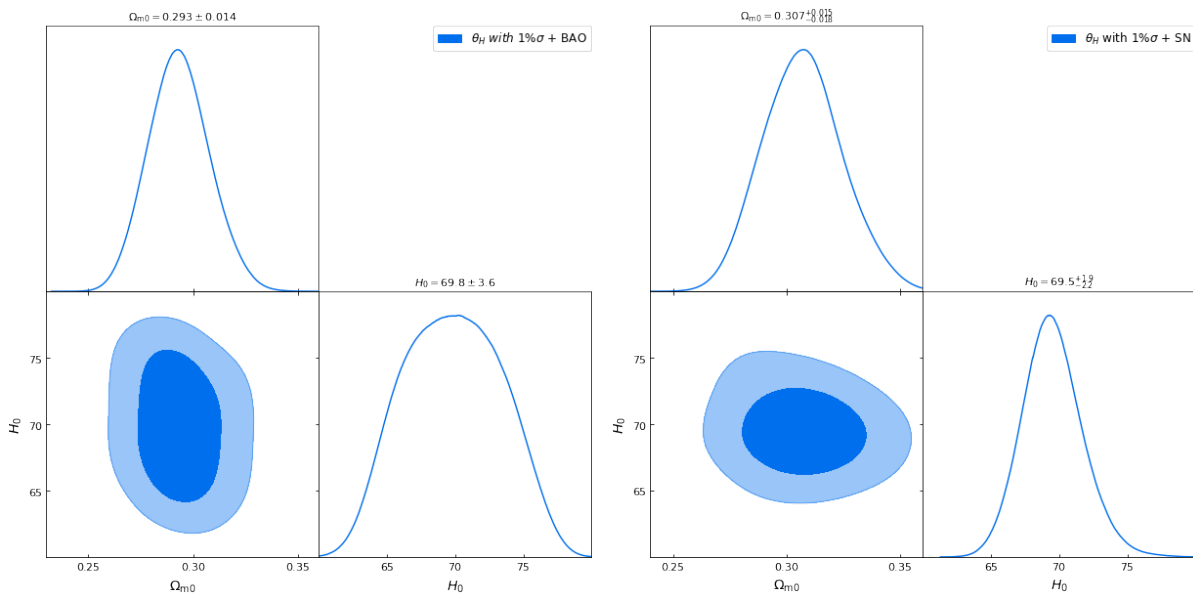


FIG. 6: Marginalized posteriors on  $\Omega_{m0}$  and  $H_0$  from the combination of the simulated  $\theta_H$  data assuming 1% precision with BAO (left) and SN (right).

SN data, resulting in  $H_0 = 69.5^{+1.9}_{-2.2}$  km.s $^{-1}$ .Mpc $^{-1}$  and  $\Omega_{m0} = 0.307^{+0.015}_{-0.018}$ . So, combining  $\theta_H$  with SN leads to tighter constraints on both values of  $\Omega_{m0}$  and  $H_0$ , further breaking the SN degeneracy between  $M_B$  and  $H_0$ .

It is important to remark that, in this joint analysis between  $\theta_H$  simulations with BAO or SN measurements shown in Fig. 6, the constraints on  $H_0$  and  $\Omega_{m0}$  were obtained by marginalizing over the bias parameters, rather than fixing them at the mean values – as in the Fig. 4. Consequently, the degeneracies related to BAO and SN

can be broken even more notably, since we are not making any assumption on the bias model in this case.

## V. CONCLUSIONS

The large-scale distribution of matter in the Universe has been used as a cosmological probe in many different ways. In this paper, we extended and completed the theoretical and observational studies on the

angular homogeneity scale  $\theta_H$  reported in previous papers [27, 28, 36, 37, 41]. After deriving new measurements of  $\theta_H$ , we obtained constraints on the matter density parameter and the Hubble constant from a sample of 23  $\theta_H$  data points lying in the redshift interval  $0.465 \leq z \leq 0.735$ .

Although the current constraints on  $H_0$  and  $\Omega_{m0}$  are not competitive with other probes, when combined with BAO and SN observations, the  $\theta_H$  data show a complementary behavior with those probes. The results of the joint analysis show a clear improvement in the constraints compared to those obtained with the angular homogeneity scale alone. This reassures us that  $\theta_H$  allows breaking the degeneracies that such probes have concerning  $H_0$ .

Finally, we also investigated the constraining power of a  $\theta_H$  sample with 1% uncertainty and showed that the limits (mainly) on  $\Omega_{m0}$  are significantly improved. With such precision, we also showed that it is possible to improve further the degeneracy breaking on the Hubble

constant by combining SN and BAO observations with  $\theta_H$  data.

### Acknowledgements

The authors thank Uendert Andrade for useful discussions. XS is supported by the Coordenação de Aperfeiçoamento de Pessoal de Nível Superior (CAPES) - PhD fellowship. CB acknowledges financial support from Fundação à Pesquisa do Estado do Rio de Janeiro (FAPERJ) - Postdoc Nota 10 (PDR10) fellowship. RSG thanks financial support from FAPERJ grant No. 260003/005977/2024 - APQ1. JSA is supported by CNPq grant No. 307683/2022-2 and FAPERJ grant No. 259610 (2021). This work was developed thanks to the use of the National Observatory Data Center (CPDON).

- 
- [1] N Aghanim, Y Akrami, M Ashdown, J Aumont, C Bacigalupi, M Ballardini, AJ Banday, RB Barreiro, N Bartolo, S Basak, et al. Planck 2018 results-vi. cosmological parameters (corrigendum). *Astronomy & Astrophysics*, 652:C4, 2021.
  - [2] Dillon Brout et al. The Pantheon+ Analysis: Cosmological Constraints. *Astrophys. J.*, 938(2):110, 2022.
  - [3] Shadab Alam et al. Completed SDSS-IV extended Baryon Oscillation Spectroscopic Survey: Cosmological implications from two decades of spectroscopic surveys at the Apache Point Observatory. *Phys. Rev. D*, 103(8):083533, 2021.
  - [4] T. M. C. Abbott et al. Dark Energy Survey Year 3 results: Cosmological constraints from galaxy clustering and weak lensing. *Phys. Rev. D*, 105(2):023520, 2022.
  - [5] Mathew S. Madhavacheril et al. The Atacama Cosmology Telescope: DR6 Gravitational Lensing Map and Cosmological Parameters. *Astrophys. J.*, 962(2):113, 2024.
  - [6] Xiangchong Li et al. Hyper Suprime-Cam Year 3 results: Cosmology from cosmic shear two-point correlation functions. *Phys. Rev. D*, 108(12):123518, 2023.
  - [7] Steven Weinberg. The Cosmological constant problems. 5 2000.
  - [8] Eleonora Di Valentino, Olga Mena, Supriya Pan, Luca Visinelli, Weiqiang Yang, Alessandro Melchiorri, David F. Mota, Adam G. Riess, and Joseph Silk. In the realm of the Hubble tension—a review of solutions. *Class. Quant. Grav.*, 38(15):153001, 2021.
  - [9] A. G. Adame et al. DESI 2024 VI: Cosmological Constraints from the Measurements of Baryon Acoustic Oscillations. 4 2024.
  - [10] R. Calderon et al. DESI 2024: Reconstructing Dark Energy using Crossing Statistics with DESI DR1 BAO data. 5 2024.
  - [11] Marina Cortês and Andrew R. Liddle. Interpreting DESI’s evidence for evolving dark energy. 4 2024.
  - [12] Purba Mukherjee and Anjan Ananda Sen. Model-independent cosmological inference post DESI DR1 BAO measurements. 5 2024.
  - [13] Chris Clarkson and Roy Maartens. Inhomogeneity and the foundations of concordance cosmology. *Class. Quant. Grav.*, 27:124008, 2010.
  - [14] Roy Maartens. Is the Universe homogeneous? *Phil. Trans. Roy. Soc. Lond. A*, 369:5115–5137, 2011.
  - [15] Chris Clarkson. Establishing homogeneity of the universe in the shadow of dark energy. *Comptes Rendus Physique*, 13:682–718, 2012.
  - [16] Pavan Kumar Aluri, Paolo Cea, Pravabati Chingambam, Ming-Chung Chu, Roger G Clowes, Damien Hutsemékers, Joby P Kochappan, Alexia M Lopez, Lang Liu, Niels C M Martens, C J A P Martins, Konstantinos Migkas, Eoin Ó Colgáin, Pratyush Pranav, Lior Shamir, Ashok K Singal, M M Sheikh-Jabbari, Jenny Wagner, Shao-Jiang Wang, David L Wiltshire, Shek Yeung, Lu Yin, and Wen Zhao. Is the observable universe consistent with the cosmological principle? *Classical and Quantum Gravity*, 40(9):094001, April 2023.
  - [17] S. W. Hawking and G. F. R. Ellis. *The Large Scale Structure of Space-Time*. Cambridge Monographs on Mathematical Physics. Cambridge University Press, 1973.
  - [18] Steven Weinberg. *Cosmology*. 2008.
  - [19] David W. Hogg, Daniel J. Eisenstein, Michael R. Blanton, Neta A. Bahcall, J. Brinkmann, James E. Gunn, and Donald P. Schneider. Cosmic homogeneity demonstrated with luminous red galaxies. *Astrophys. J.*, 624:54–58, 2005.
  - [20] Prakash Sarkar, Jaswant Yadav, Biswajit Pandey, and Somnath Bharadwaj. The scale of homogeneity of the galaxy distribution in SDSS DR6. *Mon. Not. Roy. Astron. Soc.*, 399:L128–L131, 2009.
  - [21] Morag Scrimgeour et al. The WiggleZ Dark Energy Survey: the transition to large-scale cosmic homogeneity. *Mon. Not. Roy. Astron. Soc.*, 425:116–134, 2012.
  - [22] Biswajit Pandey. A method for testing the cosmic homogeneity with Shannon entropy. *Mon. Not. Roy. Astron. Soc.*, 430:3376, 2013.
  - [23] Biswajit Pandey and Suman Sarkar. Testing homogeneity in the Sloan Digital Sky Survey Data Release Twelve



- with Shannon entropy. *Mon. Not. Roy. Astron. Soc.*, 454(3):2647–2656, 2015.
- [24] Suman Sarkar and Biswajit Pandey. An information theory based search for homogeneity on the largest accessible scale. *Mon. Not. Roy. Astron. Soc.*, 463(1):L12–L16, 2016.
- [25] Pierre Laurent et al. A  $14 h^{-3} \text{ Gpc}^3$  study of cosmic homogeneity using BOSS DR12 quasar sample. *JCAP*, 11:060, 2016.
- [26] Pierros Ntelis et al. Exploring cosmic homogeneity with the BOSS DR12 galaxy sample. *JCAP*, 06:019, 2017.
- [27] R. S. Gonçalves, G. C. Carvalho, C. A. P. Bengaly, J. C. Carvalho, and J. S. Alcaniz. Measuring the scale of cosmic homogeneity with SDSS-IV DR14 quasars. *Mon. Not. Roy. Astron. Soc.*, 481(4):5270–5274, 2018.
- [28] Rodrigo S. Gonçalves, Gabriela C. Carvalho, Uendert Andrade, Carlos A. P. Bengaly, Joel C. Carvalho, and Jailson Alcaniz. Measuring the cosmic homogeneity scale with SDSS-IV DR16 Quasars. *JCAP*, 03:029, 2021.
- [29] Yigon Kim, Chan-Gyung Park, Hyerim Noh, and Jaichan Hwang. CMASS galaxy sample and the ontological status of the cosmological principle. *Astron. Astrophys.*, 660:A139, 2022.
- [30] Francesco Sylos Labini, Nikolay L. Vasilyev, Yuriy V. Baryshev, and Martin Lopez-Corredoira. Absence of anti-correlations and of baryon acoustic oscillations in the galaxy correlation function from the Sloan Digital Sky Survey DR7. *Astron. Astrophys.*, 505:981–990, 2009.
- [31] Francesco Sylos Labini. Very large scale correlations in the galaxy distribution. *EPL*, 96(5):59001, 2011.
- [32] Chan-Gyung Park, Hwasu Hyun, Hyerim Noh, and Jaichan Hwang. The cosmological principle is not in the sky. *Mon. Not. Roy. Astron. Soc.*, 469(2):1924–1931, 2017.
- [33] Asta Heinesen. Cosmological homogeneity scale estimates are dressed. *JCAP*, 10:052, 2020.
- [34] D. Alonso, A. Bueno belloso, F. J. Sánchez, J. García-Bellido, and E. Sánchez. Measuring the transition to homogeneity with photometric redshift surveys. *Mon. Not. Roy. Astron. Soc.*, 440(1):10–23, 2014.
- [35] David Alonso, Ana Isabel Salvador, Francisco Javier Sánchez, Maciej Bilicki, Juan García-Bellido, and Eusebio Sánchez. Homogeneity and isotropy in the Two Micron All Sky Survey Photometric Redshift catalogue. *Mon. Not. Roy. Astron. Soc.*, 449(1):670–684, 2015.
- [36] R. S. Gonçalves, G. C. Carvalho, C. A. P. Bengaly, J. C. Carvalho, A. Bernui, J. S. Alcaniz, and R. Maartens. Cosmic homogeneity: a spectroscopic and model-independent measurement. *Mon. Not. Roy. Astron. Soc.*, 475(1):L20–L24, 2018.
- [37] Uendert Andrade, Rodrigo S. Gonçalves, Gabriela C. Carvalho, Carlos A. P. Bengaly, Joel C. Carvalho, and Jailson Alcaniz. The angular scale of homogeneity with SDSS-IV DR16 luminous red galaxies. *JCAP*, 10:088, 2022.
- [38] Pierros Ntelis, Anne Ealet, Stephanie Escoffier, Jean-Christophe Hamilton, Adam James Hawken, Jean-Marc Le Goff, James Rich, and Andre Tilquin. The scale of cosmic homogeneity as a standard ruler. *JCAP*, 12:014, 2018.
- [39] Pierros Ntelis, Adam James Hawken, Stephanie Escoffier, Anne Ealet, and Andre Tilquin. Cosmological constraints from cosmic homogeneity. 4 2019.
- [40] Savvas Nesseris and Manuel Trashorras. Can the homogeneity scale be used as a standard ruler? *Phys. Rev. D*, 99(6):063539, 2019.
- [41] Xiaoyun Shao, Rodrigo S. Gonçalves, Carlos A. P. Bengaly, Uendert Andrade, Gabriela C. Carvalho, and Jailson Alcaniz. Can the angular scale of cosmic homogeneity be used as a cosmological test? *Eur. Phys. J. C*, 84(7):655, 2024.
- [42] Kyle S Dawson, David J Schlegel, Christopher P Ahn, Scott F Anderson, Éric Aubourg, Stephen Bailey, Robert H Barkhouser, Julian E Bautista, Alessandra Beifiori, Andreas A Berlind, et al. The baryon oscillation spectroscopic survey of sdss-iii. *The Astronomical Journal*, 145(1):10, 2012.
- [43] Shadab Alam, Franco D Albareti, Carlos Allende Prieto, Friedrich Anders, Scott F Anderson, Timothy Anderton, Brett H Andrews, Eric Armengaud, Éric Aubourg, Stephen Bailey, et al. The eleventh and twelfth data releases of the sloan digital sky survey: final data from sdss-iii. *The Astrophysical Journal Supplement Series*, 219(1):12, 2015.
- [44] Daniel J Eisenstein, David H Weinberg, Eric Agol, Hiroaki Aihara, Carlos Allende Prieto, Scott F Anderson, James A Arns, Éric Aubourg, Stephen Bailey, Eduardo Balbinot, et al. Sdss-iii: Massive spectroscopic surveys of the distant universe, the milky way, and extra-solar planetary systems. *The Astronomical Journal*, 142(3):72, 2011.
- [45] Kyle S Dawson, Jean-Paul Kneib, Will J Percival, Shadab Alam, Franco D Albareti, Scott F Anderson, Eric Armengaud, Éric Aubourg, Stephen Bailey, Julian E Bautista, et al. The sdss-iv extended baryon oscillation spectroscopic survey: overview and early data. *The Astronomical Journal*, 151(2):44, 2016.
- [46] D Alonso, A Bueno Belloso, FJ Sánchez, J García-Bellido, and E Sánchez. Measuring the transition to homogeneity with photometric redshift surveys. *Monthly Notices of the Royal Astronomical Society*, 440(1):10–23, 2014.
- [47] Martín Crocce, Anna Cabré, and Enrique Gaztanaga. Modelling the angular correlation function and its full covariance in photometric galaxy surveys. *Monthly Notices of the Royal Astronomical Society*, 414(1):329–349, 2011.
- [48] S Basilakos, M Plionis, and C Ragone-Figueroa. The halo mass-bias redshift evolution in the  $\lambda$ cdm cosmology. *The Astrophysical Journal*, 678(2):627, 2008.
- [49] Pierros Ntelis, Anne Ealet, Stephanie Escoffier, Jean-Christophe Hamilton, Adam James Hawken, Jean-Marc Le Goff, James Rich, and Andre Tilquin. The scale of cosmic homogeneity as a standard ruler. *Journal of Cosmology and Astroparticle Physics*, 2018(12):014, 2018.
- [50] Antony Lewis, Anthony Challinor, and Anthony Lasenby. Efficient computation of cosmic microwave background anisotropies in closed friedmann-robertson-walker models. *The Astrophysical Journal*, 538(2):473, 2000.
- [51] Stephen D Landy and Alexander S Szalay. Bias and variance of angular correlation functions. *Astrophysical Journal*, Part 1 (ISSN 0004-637X), vol. 412, no. 1, p. 64–71., 412:64–71, 1993.
- [52] Micael Jarvis, Gary Bernstein, and Bhuvnesh Jain. The skewness of the aperture mass statistic. *Monthly Notices of the Royal Astronomical Society*, 352(1):338–352, 2004.
- [53] AG Adame, J Aguilar, S Ahlen, S Alam, DM Alexander, M Alvarez, O Alves, A Anand, U Andrade, E Armen-

- gaud, et al. Desi 2024 vi: Cosmological constraints from the measurements of baryon acoustic oscillations. *arXiv preprint arXiv:2404.03002*, 2024.
- [54] David Camarena and Valerio Marra. The tension in the absolute magnitude of Type Ia supernovae. 7 2023.
- [55] Ashley J Ross, Lado Samushia, Cullan Howlett, Will J Percival, Angela Burden, and Marc Manera. The clustering of the sdss dr7 main galaxy sample–i. a 4 per cent distance measure at  $z = 0.15$ . *Monthly Notices of the Royal Astronomical Society*, 449(1):835–847, 2015.
- [56] Florian Beutler, Chris Blake, Matthew Colless, D Heath Jones, Lister Staveley-Smith, Lachlan Campbell, Quentin Parker, Will Saunders, and Fred Watson. The 6df galaxy survey: baryon acoustic oscillations and the local hubble constant. *Monthly Notices of the Royal Astronomical Society*, 416(4):3017–3032, 2011.
- [57] Shadab Alam, Metin Ata, Stephen Bailey, Florian Beutler, Dmitry Bizyaev, Jonathan A Blazek, Adam S Bolton, Joel R Brownstein, Angela Burden, Chia-Hsun Chuang, et al. The clustering of galaxies in the completed sdss-iii baryon oscillation spectroscopic survey: cosmological analysis of the dr12 galaxy sample. *Monthly Notices of the Royal Astronomical Society*, 470(3):2617–2652, 2017.
- [58] Shadab Alam, Marie Aubert, Santiago Avila, Christophe Balland, Julian E Bautista, Matthew A Bershady, Dmitry Bizyaev, Michael R Blanton, Adam S Bolton, Jo Bovy, et al. Completed sdss-iv extended baryon oscillation spectroscopic survey: Cosmological implications from two decades of spectroscopic surveys at the apache point observatory. *Physical Review D*, 103(8):083533, 2021.
- [59] Daniel Moshe Scolnic, DO Jones, A Rest, YC Pan, R Chornock, RJ Foley, ME Huber, R Kessler, Gautham Narayan, AG Riess, et al. The complete light-curve sample of spectroscopically confirmed sne ia from pan-starrs1 and cosmological constraints from the combined pantheon sample. *The Astrophysical Journal*, 859(2):101, 2018.